Design, Modeling, and Thermal Validation of an Electric Resistance Furnace for High-Temperature Applications

Malik Sarmad Zahid[*], Afaque Ahmed Hayat[†], Asad Ullah[‡], Arshad Ali Khan[§], Afnan Haider Khan[**]

Abstract

This paper describes the design, analytical modeling, and numerical thermal analysis of an electric resistance furnace intended to reach 1200°C. The geometry of a hexagonal heating chamber was used because it provides the highest level of effective heating volume and allows the use of commercially available lightweight refractory bricks. The one-dimensional steady-state analytical heat-transfer model and Finite Element Thermal Analysis (FEA) were performed with ANSYS APDL and ANSYS Workbench. The prediction by the analytical model showed an external wall temperature of about 404 K in the uninsulated furnace, which was too high, indicating excessive heat loss and that minute operating temperature conditions were not safe; the numerical results indicated the same temperature of 395 K with an error of 2.22%. This was counteracted by adding a 40 mm thick insulation layer in the form of ceramic fibers, which led to a reduction in the predicted analytical and numerical results of the external surface temperatures to 356 K and 326 K, respectively, and a standard deviation of 8.42. The insulated design exhibited a decreased amount of heat loss by about 45% and greatly enhanced the retention of heat in the heating chamber. The furnace was expected to reach a temperature of 1200°C in the furnace body in a period of one hour in operation, while keeping the exterior body of the furnace close to ambient temperature. The analytical and numerical results are very close and justify the proposed furnace design and prove the effectiveness of ceramic fiber insulation use in the high-temperature electric furnace.

Keywords: Resistance Furnace, Heating Chamber, Joule Heating, Indirect Heating, Melting, Heat Treatment.

Introduction

In a Direct Current Electric Arc Furnace (DC-EAF), the authors performed parametric study to determine the effect of arc gap distance, gas density and total electric current on arc stability, impingement depth, and

[*]Department of Mechanical Engineering, University of Engineering & Technology Mardan, Mardan 23200, Pakistan, sarmad@uetmardan.edu.pk

[†]Department of Mechanical Engineering, University of Engineering & Technology Mardan, Mardan 23200, Pakistan, afaqueahmedhayat@gmail.com

[‡]Department of Mechanical Engineering, University of Engineering & Technology Mardan, Mardan 23200, Pakistan, asad@uetmardan.edu.pk

[§]Corresponding Author: Department of Mechanical Engineering, University of Engineering & Technology Peshawar-Nowshera Campus, Nowshera 24100, Pakistan, engrarshad@uetpeshawar.edu.pk

[**]Department of Mechanical Engineering, University of Engineering & Technology Mardan, Mardan 23200, Pakistan, afnan@uetmardan.edu.pk

mix of liquid metals. They came up with the conclusion that the most important parameter was the total applied current which directly determined the penetration depth and the stirring intensity in the bath. Although gas density greatly influenced the arc velocity profiles, it did not greatly influence impingement depth and a constant density assumption was justifiable to improve computational efficiency (Al-Nasser et al., 2021).

The study provide an exhaustive review of the simulation and numeric modeling methods of electric arc furnaces and their processes, stating that they are very crucial in the steel industry The authors analytically review different modeling methods such as thermodynamics-based models, data-driven models, and hybrid models and explain how they have been used in explaining the processes of heat transfer, chemical reactions, and fluid dynamics in Electric Arc Furnaces (EAFs). They examine various operation steps, such as charging, melting, refining, removal of the slag, and tapping, as well as the use of energy and issues of balance (Abadi et al., 2024).

The authors numerically researched a new water-cooled design of an electric arc furnace roof by a finite element analysis method to evaluate heat transfer and temperature field. Their design included the use of two materials, copper and alumina brick, which had the water pipes inbuilt and actively cooled. Findings have shown that decreasing the thermal conductivity of the brick led to a decrease in the temperature of the top surface of the brick, but when the conductivity decreased by 380 to 2.9 W/m 0 °C, the surface temperature dropped to 84.4 °C. Also, geometry made of bricks in a rectangular shape was more effective in maintaining lower temperatures on the roofs as compared to wedge-shaped buildings. (Assad et al., 2021). In another study, simulations were conducted to explore the application of the Al_2O_3/Water nanofluid as a coolant in the wall cooling panels of an arc steelmaking furnace that operated by electricity. Their Computational Fluid Dynamics (CFD) experiment compared the temperature performance of pure water to nanofluids at 3, 4, and 5% particle concentration in actual operating conditions. When the concentration of nanofluid was increased to 5%., it lowered the maximum temperature of the hot-side wall by 14.4%, and evenly distributed the temperature across the surface, reducing the gap between the highest and average temperature to 12˚C. It was determined in the study that nanofluid is an efficient technique to fight thermal stress, increase the life of panels and enhance cooling in general (Babadi et al., 2023).

In their work, a quantitative analysis of the influence of ambient temperature, air velocity, slag thickness, and cover thickness of the furnace on Hot Metal (HM) temperature drop was analyzed using a 50-minute

transport period. It was found that the slag thickness was the most influential single variable, giving the temperature a drop of about 55.2 ˚C with slag, though the drop of the temperature to about 10.3˚C when the slag thickness was 150 mm thick. Ambient temperature and air velocity did not influence the uncovered HM significantly, but air velocity influenced the uncovered HM greatly with slag (Chen et al., 2024).

The authors have analyzed the present situation and outlook of electric arc furnace scrap steel preheating technology, which is one of the most important techniques to enhance the scrap usage, lower the energy consumption, and decrease the pollution of green steel making. The authors discussed three mainstream technologies, whereby continuous feeding and flue gas heat exchange is applied to reduce power consumption drastically, but the technologies are expensive and demand cumbersome equipment; the double-shell EAF, where alternating smelting and waste heat circulation is used, resulting in 350-400 kWh energy consumption but has to adopt dioxin control and scrap impurity treatment issues; and the shaft-type EAF, known to deliver high preheating efficiency and low emissions but has to handle the challenge of the quality of raw materials (Du et al., 2025).

In another study, a numerical method of the calculation of temperatures distribution and energy flows in an electric furnace is discussed. They obtain a nonlinear diffusion equation using a model with temperature-dependent thermal properties, which they solve by finite difference discretization in 2D using Scientific Laboratory (SCILAB) scripts, using the net radiation method by Hotle to code a radiative exchange. Design and development of a ceramic material to be used in the 100% electric arc furnace steel slag as a single feedstock with high-temperature thermal energy storage applications. The authors examined the effect of process parameters and concluded that the best properties were obtained when the heat-treated slag powders were pressed at a pressure of 300 MPa and fired at 1300˚C in the presence of a static air atmosphere for 8 hours. The resulting ceramic was found to have a bulk density of 3.08 g/cm^3, water absorption of 1.2, specific heat capacity values in the range of 1026 to 1216 J/kg-K at 200-600 ˚C, and thermal conductivity in the range of 1.37-1.53 W/m.K (Ferber et al., 2022).

The study examined the design and real-time control of a new electric furnace with three-dimensional heating, which had heaters and temperature sensors on all six interior surfaces. Based on the results of the Ziegler-Nichols tangent technique, they learned the heating characteristics of the furnace and identified optimal gain factors of Proportional (P), Proportional-Integral (PI), and Proportional-Integral-Derivative (PID) controllers. Their experimental findings showed that homogeneous heating

would be attained only in the case when there was an active control of all six panels. In addition, the PI and PID controllers brought about the system with a maximum steady-state error of 1.3˚C, which confirmed the accuracy of the model used in the system as well as the success of the adopted control strategy. (Guney et al., 2025). The design of a contemporary temperature control system of an industrial electric furnace using a modified optimization method was studied. They offered the adaptive control scheme wherein the PID controller gains are on-line tuned by an Enhanced Whale Optimization Algorithm (EWOA) with a modification of the Balloon Effect (BE). This method came about to overcome the shortcomings of the traditional PID controllers in dealing with variations in system parameters and step interferences. Their simulation data revealed that the EWOA+BE approach presented a better dynamic behavior (in terms of the best overshoot, rise time, and settling time) (Hussein et al., 2022).

In one study, the enhancement of the heating capability of an electric furnace in the special case of aluminum waste management in a vocational workshop was discussed. They re-engineered the heating system with the help of the Engineering Design Process (EDP) model by introducing a dual-heating element design using Kanthal resistance wire, a PID controller to adjust temperature more accurately, and use of proper electrical parts such as a solid-state relay. Their experiment findings showed that the time taken to heat had reduced drastically, and the system was able to reach a temperature of 650°C in a period of about 5 to 7 minutes, as compared to the old, ineffective system. (Huzaidi et al., 2023).

The authors evaluated and constructed two computationally efficient View Factor (VF) computations in the modeling of a process inside an EAF process or configuration that is vital in modeling radiative heat transmission accurately. The authors contrasted a Monte Carlo (MC) statistical method with a method involving analytic approximation and justified it and both methods against high-fidelity CFD simulations. Their analysis revealed that the MC method was more accurate, but the analytical method was faster and accurate enough as a substitute for the former one, so it would be appropriate for online process optimization and real- time solutions (Hay et al., 2021).

In the study, the authors created a dynamic and first-principles thermophysical model of an EAF to optimize and Model Predictively Control (MPC) in real time. The model incorporates both mass and energy balance with a detailed description of inner and outer steel control volumes, slag phases, and furnace equipment, and applies ordinary differential equations to trace state variables. The authors used MPC simulations to show that optimized electrical power profiles could save a

specific energy use of 1-2 %, and that projected energy savings of 15.75 kWh /ton in single-basket heat could be saved (Jawahery et al., 2021). The study revealed the recovery of waste heat in metal pools that had to be used in the cooling of High-Carbon Ferrochrome (HC-FeCr) in the electric arc furnaces The authors proposed and developed the system with the use of a heat exchanger fitted under the metal pools to warm the circulating water between 15-20 ˚C to a target temperature of 85-90 ˚C, therefore, decreasing the use of fossil fuel and carbon emission. Economic analysis showed that using such a system to heat 10 m^3 of water conserves 813 kWh of energy, which is the same amount of coal burnt 195 kg, or natural gas burned 91 m^3, which would save a lot of carbon (Kishore et al., 2025).

In the article, numerical simulation and structural optimization of the heating process in a vacuum sintering electric furnace, whereby a three-dimensional model was developed, and a special temperature voltage feedback control program was written. It was determined in their analysis that there was considerable thermal hysteresis between the heating tube and graphite cylinder in the heating stage, which was measured by a dimensionless difference in hysteresis temperature, whose maximum was at 0.4. The model was tested using experimental data, and the relative errors were found to be within 4%. The paper shows that these optimizations have the potential to improve the operation of a furnace, improve the life of its components, and offer viable information to design and operation of industrial vacuum sintering furnaces (Li et al., 2024).

A three-stage 12 MVA electric arc furnace model was designed in terms of a mixed electromagnetic-thermal model and operational data in real time. They simulated electric field gradient distributions, current density, and melt movement in their study, showing high levels of current concentration around electrodes and related patterns of convection. The authors came to the conclusion that by combining such simulations with real data, it is possible to create a digital twin of the furnace and predict the best operating conditions and diagnose failures. (Lee et al., 2023). The authors introduce a theoretical and practical research about heat transfer in the electric arc furnace, flare furnace and combustion chamber. The author develops five main laws that are used in the radiation of cylindrical and spherical volumes of gas, which allows simplified and correct calculation of radiative heat fluxes of complex industrial systems. According to these concepts, Makarov came up with detailed methods for modeling heat transfer in electric arc furnaces in steelmaking, flare heating furnaces, steam boiler furnaces, and gas turbine combustion chutes (Makarov et al., 2020).

In another study, the melting of Hydrogen Direct Reduced Iron (HDRI) pellets was examined, which had a reduction degree of 68% and

100% in an electric arc furnace on a laboratory scale. Their research found that the presence of iron oxide-rich slag had a strong effect on arc movement and prevented the evaporation of iron, and the effect of in-situ monitoring through video and optical emission spectroscopy, which recorded the dynamics of the melt flow and slag droplets. They concluded that the major distinction in the melting behavior could be explained by the presence of iron oxide-rich slag that restrained the arc to a smaller space than the free arc movement would have resulted in a higher metallization (Pauna et al., 2025).

A comparison of the novel alkaline roasting and organic acid leaching process of electricity arc furnace dust to the traditional pyrometallurgical Waelz process was conducted using simulation and life cycle assessment of the two processes to assess the technical and environmental merits of each. The authors established that the Global Warming Potential (GWP) of the novel process (7.48 g of CO_2 per kg of zinc) was greater than that of the Waelz process (4.71 g of CO_2), when dust containing 33% zinc was used. The new process was more competitive at the lower zinc contents; at 12% zinc dust, the GWP values of the novel process were 6.31 kg CO_2-eq (Rinne et al., 2022)

To study the heat fluxes in a pusher furnace during slab heating in the steel production process, the authors designed and used a mathematical model. The model was utilized to measure the performance of the furnace prior to reconstruction and after reconstruction, which involved additions like better insulation, renovated burner systems, and the flue gas flow path. The outcomes indicated that the reconstructed furnace had an improved uniform temperature distribution through the entire slab thickness and also saved an order of magnitude on the consumption of specific energy, with the calculated heat fluxes falling to as little as 65% at some locations (Varga et al., 2023).

In a simulation study, a full tap-to-tap cycle in a 150-ton AC EAF was simulated using industrial data, which was provided in NLMK Indiana. To verify their built-in CFD solver, which is the integrative model of scrap melting, electric arc, and coherent jet modeling, they compared the simulated electrode status and melting rates with the real data of the working operation. The findings indicated a high degree of correspondence with the electrode position estimates falling within a 5 percent error range and the bore-in rates of the initial scrap bucket falling within 3% of the industrial values. The second bucket predictions were, however, less accurate, especially through unmodeled arc instabilities because of scrap cave-ins (Wang et al., 2025).

Most research that has been conducted shows that the arc furnace at large scales has been analyzed the arc furnace in terms of isolated

numerical and control-based optimization. There is still very limited experimental research on heating uniformity, transient thermal behavior, and system-level performance improvement of small-to-medium scale electric furnaces under realistic operating environments. Furthermore, the experimentally supported furnace design modifications that directly relate to heating configuration, temperature distribution, and energy efficiency have not been experimentally validated despite the potential benefits that have been demonstrated by using advanced numerical models and optimization-based controllers. Specifically, the productiveness of the heater arrangement, temperature control in real-time, and the subsequent heating rate enhancement have not been adequately measured in the literature. Thus, there is an apparent gap in experimentally showing how design level changes, together with controlled heating measures, can increase thermal uniformity, decrease heating time, and generally make furnace performance better. This gap is addressed in the present work through analytical modeling and numerical thermal analysis of an electric resistance furnace using finite element simulation, which justifies an increase in efficiency and practical utility in creating a sustainable processing of metals. Even though the EAF is popular in industrial steel production since it can produce extremely high temperatures by arc discharge, the current work concentrates on an electric resistance furnace that employs Joule heating in resistive elements to perform high-temperature processing and thermal performance experimentation on a controlled scale.

Methodology and Fabrication

Conceptual Modeling

At this stage, several conceptual models are formulated on the basis of the literature review. Every model has its pros and cons. The conceptual design is the very 1st step of the project design. The first conceptual is rejected due to its high power, and its shape because that type of model is already available in market, as shown in Figure 1(a) and its temperature control unit might be heat up due to conduction. Then another conceptual model was developed as shown in Figure 1(b), it is also rejected due to its small heating space consuming more power due to its three turns of coil, and it is very expensive in the market. Another conceptual model as shown in Figure 1(c) failed because it has below its control unit where high temperatures and the weight of the furnace might damage the control unit. Then the fourth furnace design, as shown in Figure 1(d) has a very small heating chamber and has more coil turns, which is why it's rejected. The one that is selected, as shown in Figure 2,

has a big heating chamber. It is a unique design in which the thickness of the bricks is more so heat will be there for more time in the heating chamber. Also, its manufacturing is easy, and rectangular fire bricks are easily available in the market.

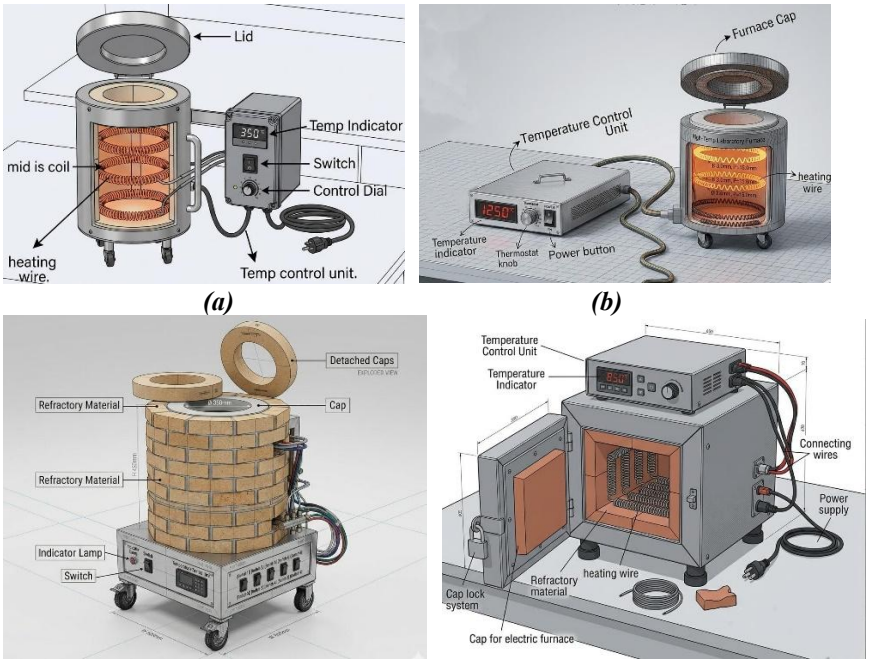

Figure 1: Conceptual design configurations of the electric furnace during the initial design stage.

CAD Modeling

The entire setup is made up of all the manufactured bricks fitted in place to create the structure of the furnace where the heating coil is placed either inside the walls of the bricks or installed within the pre-carved ribs so that it supports itself and allows even distribution of the heat, as shown in Figure 3. The furnace chamber has a crucible in the middle that is thermally insulated with high-temperature ceramic fiber in order to reduce the amount of heat loss to the surroundings and enhance the efficiency of energy usage. The insulated furnace is outwardly covered by a stainless-steel sheet, which serves as mechanical protection and durability, and the rods are angle-shaped irons, which are employed to give structural strength and rigidity. Lastly, the furnace system is installed with a Temperature Control Unit to allow the fine control and monitoring of the operating temperature.

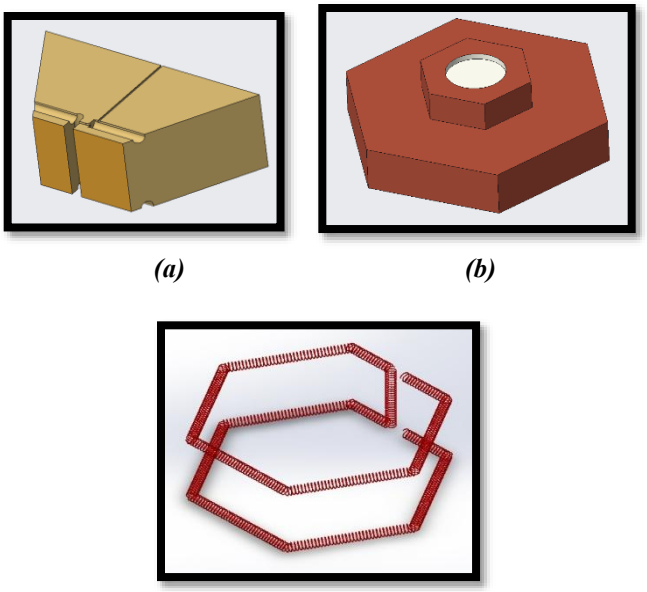

(a) *(b)*

(c)

Figure 2: Conceptual components design of electric furnace (a) Double slotted brick, (b) Head, and (c) Heating coil.

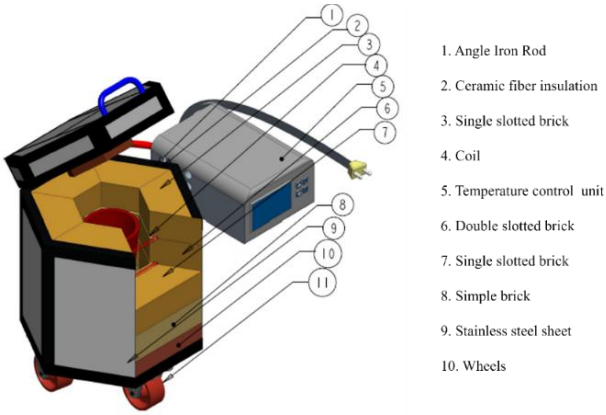

Figure 3: Complete assembly of the electric furnace.

Electric resistance heating is used for heating solids, liquids and gases by contact, natural and forced convection, and radiation in almost every conceivable area of industry. The electrical heating furnace is planned to operate up to 1300 °C. Therefore, Kanthal heating element (Kanthal A-1 wire) is selected as the heating wire for the electrical heating furnace. Physical and mechanical properties of the wire are illustrated in

Table 1. It is a ferrite-iron-chromium-aluminum alloy. It is a resistance-based electrical heating wire, which can be used to heat things to 1400°C. This material has high electrical resistivity and very good oxidation resistance. It is widely used as an electrical heating element in high-temperature furnaces for heat treatment, ceramics, glass, steel, and electronics industries. The hexagonal heating chamber was chosen since it offers a higher effective heating volume, whilst having a small size. This geometry helps to distribute the heat more uniformly and eliminate sharp corners, minimize local thermal gradients, and enhance effective convective and conductive heat transfer in the chamber. The hexagonal arrangement enables the refractory bricks to interlock properly, which increases their mechanical stability and their ability to withstand thermal stresses when operating in high temperatures.

Table 1: Physical and mechanical properties of Kanthal wire.

Properties	Values
Operating temperature in air	1400°C
Nominal composition	Cr=22, Al=58
Temperature factor of resistivity at 1200 °C, C_t	1.04
Melting point °C	1500
Tensile strength MPa	680
Yield Strength, MPa	584
Elongation at rupture %	20
Emissivity fully oxidized condition	0.7

Refractory bricks or fire brick is a block of refractory ceramic material used in the lining of furnaces and kilns. In this study, Corundum Mullite bricks are selected because of their low thermal conductivity, which can hold heat in the furnace for a longer time, and high temperature resistance. Table 2 shows the specifications of bricks.

Table 2: Properties of refractory bricks.

Properties	Values
Maximum Temperature, °C	1430
Density, g/cm^3	0.9
Modulus of Rupture, MPa	1.4
Thermal Conductivity at 1200°C, W/m^2k	0.4
Crushing strength, MPa	1.6
Alumina, AI_2O_3 , %	58
Iron(III) oxide, Fe_2O_3, %	0.8

To further enhance thermal efficiency, ceramic fiber is used as an insulating product because of its low thermal mass and low thermal conductivity. Its high thermal shock resistance makes it suitable for applications where traditional refractories cannot be used. The properties of insulation are illustrated in Table 3. The frame material is mild steel (angle iron rod 3 mm thick) to support the bricks, ceramic fiber insulation,

and stainless-steel sheet. The melting process is carried out in a graphite crucible that has high conductivity, is easily available, and has a low cost.

Table 3: Properties of ceramic insulation.

Parameter	Values
Temperature, °C	1400
Al_2O_3, %	53
SiO_3, %	46
Fe_2O_3 (≦%)	0.2
Bulk Density, g/cm^3	128
Thermal Conductivity at 1000 °C, W/m-K	0.153

In the present study, constant thermal conductivity is assumed for refractory and insulation materials to simplify the model. Although conductivity varies with temperature, the variation is moderate over the operating range, causing a negligible impact on overall heat flux and temperature distribution. Temperature-dependent properties would refine local accuracy near steep gradients but do not affect the global thermal behavior.

Analytical Design

Analytical design requires developing a correct solution to a well-defined problem in a specific knowledge domain using the language of mathematics. The analysis of the thermal circuit diagrams for the furnace with and without wall insulation is presented below.

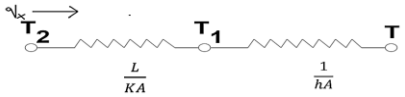

$$Q = \frac{\triangle T}{\frac{L}{K}+\frac{1}{h}} = \frac{T_2 - T}{\frac{L}{K}+\frac{1}{h}}$$

$$Q = h \triangle T = h (T_1 - T)$$

$$T_1 = \frac{Q}{h} + T$$

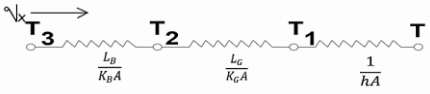

$$Q = \frac{\triangle T}{\frac{L_B}{K_B}+\frac{L_G}{K_G}+\frac{1}{h}} = \frac{T_3 - T}{\frac{L_B}{K_B}+\frac{L_G}{K_G}+\frac{1}{h}}$$

$$Q = h \triangle T = h (T_1 - T)$$

$$T_1 = \frac{Q}{h} + T_1$$

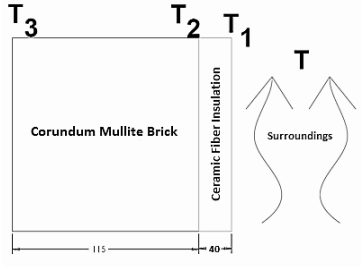

In the case of the uninsulated furnace wall, the analysis is on the basis of the one-dimensional steady-state heat conduction based on a plane wall with convectional heat loss to the environment. The thickness of the furnace wall is assumed to be 115 mm and the thermal conductivity to be 0.4 W/m 2 K whereas the external convective heat transfer coefficient is set to 35 W/m^2K which is under natural convection conditions. The temperature of the heating chamber, in the inner surface, is set to 1473 K, which is the temperature of the furnace in operation, and 298 K is the temperature of the ambient. The heat flux is obtained by modeling the system as a thermal resistance network composed of the conduction resistance in the form of the wall and the convection resistance in the form of the outer surface to be 3717.51 W/m^2K. This heat flux yields the temperature of the outer surface of the wall of the furnace as about 404.21 K, which shows that it loses a lot of the heat to the environment, and its exterior surface is not safe to touch. This finding validates the fact that without the insulation, much of the thermal energy is lost out of the furnace decreasing the efficiency and creating safety problems. The thermal conductivity of 0.153 W/m^2K of a layer of 40 mm thick ceramic fiber insulation is added to the analytical model to achieve the desired thermal performance. Modeling The furnace wall and insulation are represented by series thermal resistances in this case, external convection to the ambient.

The operating and ambient temperatures are held at the same level in order to make an equal comparison. The addition of insulation leads the overall thermal resistance of the system to a much higher value of 2034.59 W/m^2, leading to a reduction of the heat flux to 2034.59 W/m^2 instead of 3847.41 W/m2 or an approximate 45 percent decrease in the amount of heat loss. The resultant temperature of the outer surface is 356.13 K which is near ambient temperature and therefore safe to handle by human hands when in contact with a stainless-steel outer cover. The model of analysis is based on a one dimensional steady-state conduction assumption along the principal thermal gradient. Radiative heat transfer is not taken into consideration because at these temperatures and emissivity, its value is insignificant compared to that of conduction. The uniform cross-sectional geometry and boundary conditions also imply that lateral and multidimensional conduction effects are minimal, which justifies the 1D conduction approximation in order to conduct an accurate thermal analysis.

Results

Computational Fluid Dynamics (CFD) Analysis

Figure 4 represents the result of a three-dimensional temperature distribution within the electric heating chamber when air is the heat transfer medium. The inner furnace surface temperature applied as a numerical simulation boundary condition was 1473 K, which is the operating temperature of the heating chamber. The natural convection was applied on the outer face which had a coefficient of 35 W/m^2K and an ambient temperature of 298 K. These were the chosen conditions of the boundary in order to reflect realistic operating conditions of the furnace. The findings reveal that the highest temperature (1473 K) is concentrated near the heating coils and this proves that the primary source of heat generation is the resistive heating. Moving away from the coils, the temperature start decreasing monotonically towards the center of the chamber, which is the major trend of temperature.

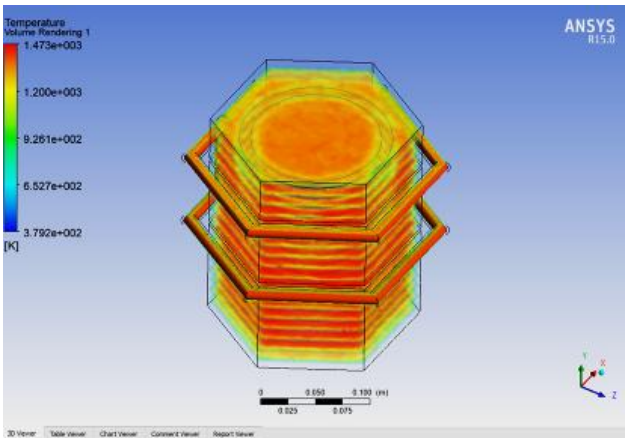

Figure 4: Temperature distribution analysis using CFD.

The progressive decrease here confirms the fact that, by conduction, the heat is initially given off to the surrounding air and returned to the center of the chamber by a natural convection process due to the presence of buoyancy. The hot air and the cooler air in the atmosphere create a continuous circulation pattern, through which the temperature field is homogenized and the thermal stratification is inhibited. The almost symmetric temperature contours indicate the uniform distribution of heat across all directions and confirm that the coils were placed optimally and the furnace was geometrically balanced. Also, the thermal insulation is efficient since relatively small temperature gradients along the walls of the furnace prove that. In general, it is evident

that the observed trend shows that there are no longer any localized areas of high temperatures in the coils, but the temperature is evenly distributed inside the heating chamber, which proves the effective volumetric heat transfer by air.

A distinct and physically relevant temperature profile is clearly observed during the transfer of heat from the heating chamber to the crucible in Figure 5. The findings reveal that the highest temperature of about 1450-1473 K occurs in the closest area of the heating coils and that the temperature decreases steadily to around 1200-1300 K at the outer air space as the heat is carried out of the source. This gradual decrease proves the fact that the thermal energy is initially carried away to the air by coils through conduction and finally to the crucible through natural convection caused by buoyancy. A steep temperature gradient (about 50-80K across the air solid interface), which marks efficient heat transfer by convection and a thermal boundary layer, is observed as the hot air pushes the cold air against the surface of the crucible. In the wall of the crucible, the temperature is gradually lowering at the outer side to between 1000 and 1100 K in the inner place, respectively, indicating that the main mode of heat transfer is the conduction via the solid material. The low temperature zone, about 950-1000 K, is experienced near the base area of the furnace with the anticipated natural convection direction of the cooler air tendencies to accumulate at the lower areas, and a small amount of heat loss is suffered through the structural supports.

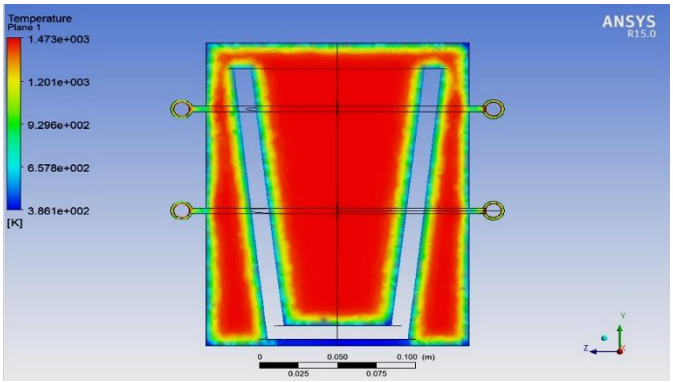

Figure 5: Heat distribution of plane.

Despite these localized reductions, the overall pattern of temperature is monotonic and symmetric. This confirms that adequate thermal energy is carried into the volume of the crucible. These numerical patterns substantiate the usefulness of air as a heat transfer medium and establish that the furnace design will provide controlled, uniform, and

predictable heating, which can be utilized in high-temperature furnace applications. The temperature field inside the system has a uniform profile, and no evident local hot spots or cool spots are observed. This indicates that there is good thermal conductivity and heat transfer within the medium, which leads to the assumption that the temperature field is homogeneous to facilitate analysis.

Finite Element Analysis of Furnace

A steady-state thermal analysis of a plane wall that represents the enclosure of the furnace. The model is made up of four nodes with Node 1 being the heating chamber, Nodes 2 and 3 being the inner and outer surfaces of the corundum mullite refractory wall of thickness 115 mm and Node 4 being the surrounding ambient environment, as shown in Figure 6. The highest temperature of 1473 K is at Node 1 which represents the desired temperature of the furnace. The difference in temperature between Node 1 and Node 2 is relatively low, which implies that the heating chamber is heating the refractory wall. It is explained by the fact that the thermal conductivity of corundum mullite is relatively high at high temperatures.

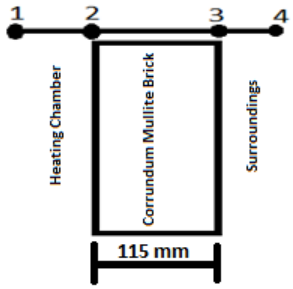

Figure 6: Representation of nodes on the plane wall.

There is a great temperature gradient between the thickness of the refractory walls between Nodes 2 and 3. In spite of such a gradient, the temperature of the outer wall surface is 395.4 K. This higher temperature on the surface signifies a high amount of heat loss to the environment and is potentially dangerous as far as human interaction is concerned. This could also mean that the external surface temperature is high, resulting in inefficient thermal containment in the furnace, resulting in consuming a lot of energy in the process. The findings indicate that a single-layered refractory wall, though structurally sound in use in high-temperature environments, is poor as far as thermal insulation is concerned. As a result,

more thermal resistance is needed to minimize the heat loss and enhance safety in the operation.

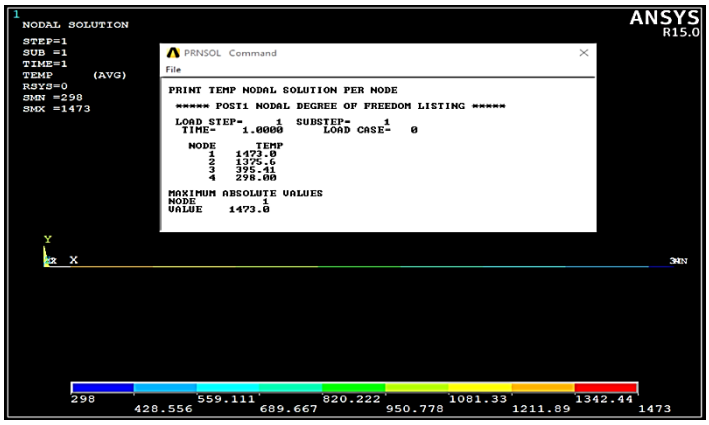

Figure 7: Numerical Results of heat transfer through plane wall.

Thermal analysis of the plane furnace wall in the absence of insulation to assess the heat loss and retention in the furnace wall under the operating conditions of high temperature is shown in Figure 7. Here, Node 1 is the heating chamber inside, Nodes 2 and 3 are the furnace wall, which has a thickness of 115 mm, respectively. Node 4 is the surrounding environment, which is subjected to ambient conditions. The nodal temperature results as presented indicate that the highest temperature of 1473 K is attained at Node 1, which is the heating chamber and confirms that the thermal loading implemented was working. At Node 2, the temperature decreases to about 1375.6 K, which means that the heat is transferred to the material of the wall of a furnace through conduction. Nevertheless, a strong decrease in temperature is noted at Node 3 and the temperature drops to 395.4 K and further to 298 K at Node 4, respectively. This temperature gradient of close to 980 K across the walls of the furnace testifies to the fact that a considerable portion of heat is being conducted across the walls of the furnace and is lost to the environment through natural convection and radiation. The thermal efficiency and human safety of Node 3 temperature level are not safe, meaning that the wall of the furnace is inadequate to maintain the heat in the chamber. These findings are clear indicators that when the furnace is not properly insulated, the furnace experiences too much heat loss, low thermal efficiency and potentially dangerous temperatures on its outer surface. Hence, insulation is critical to enhance heat loss and the safety of operation.

To overcome the heat loss experienced in the uninsulated scenario, a second thermal analysis was conducted by inserting ceramic fiber

insulation of 40 mm in thickness on top of the furnace wall. In this arrangement, Node 1 is the heating chamber, Nodes 2 and 3 are the walls of the furnace (115 mm thick). Node 4 is the layer of ceramic fiber insulation, and Node 5 is the surrounding environment, respectively. The nodal temperature values in Figure 8 indicate that the highest temperature is still 1473 K at Node 1, which confirms that the conditions of internal heating have not changed and provides a reasonable comparison to the situation with the lack of insulation. The temperature in Node 2 is noted to be around 1444.7 K, which means that a larger percentage of the heat is stored in the wall of the furnace because there is the presence of insulation. The temperature of Node 3 gradually drops to 1318 K proving controlled conductive heat transfer of the wall material as shown in Figure 9. At Node 4 the temperature drops to about 326.3 K, which is very near ambient conditions and well within the tolerable range of human interaction. Lastly, the Node 5 is at 298 K, which is an indication of insignificant heat loss into the environment. Ceramic fiber insulation is a good addition to prevent any heat transmitting to the outside surface since it forms a high thermal resistance layer. In addition, the stainless-steel outer cover also provides structural protection and secure safe surface temperature.

Figure 8: Plane wall with insulation.

Comparing the two analyses, it can be noted that insulation plays a vital role in the thermal efficiency of a furnace. In an uninsulated case, the temperature of the external wall reaches 395 K, which is considered excessively high and leads to unstable conditions of work. Conversely, with the ceramic fiber insulation, the temperature of the external surface is lowered to about 326 K, which is a decrease of about 70 K. Besides, the temperature at the inner wall area rises by 1375.6 K to 1444.7 K, which means better heat storage in the heating chamber. This affirms that

insulation plays a vital role in heat losses due to conductivity and convection, thermal efficiency, and also the safety of persons during the operations. The final findings of the Finite Element Thermal Analysis (FEA) confirm the fact that ceramic fiber insulation is necessary to keep the internal temperatures high and reduce the heat loss to the environment and ensure the thermal effectiveness and safety of the furnace design.

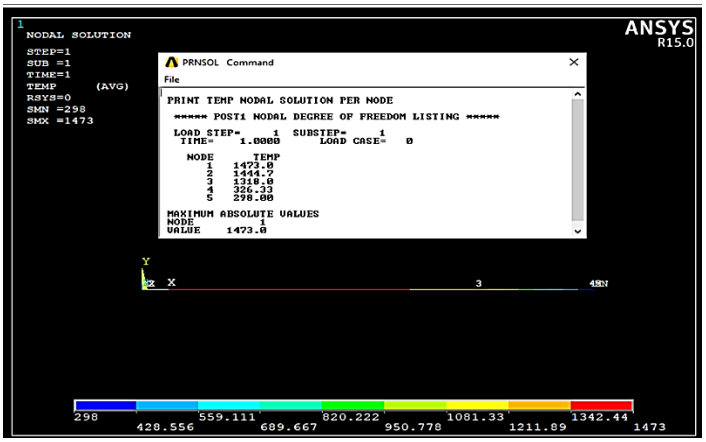

Figure 9: Numerical analysis of heat transfer through the insulated furnace.

Comparisons of Analytical and Numerical Thermal Analysis

To confirm the validity and reliability of the proposed design of the furnace wall, a detailed comparison of the analytical model and numerical (FEA-based) thermal analysis is performed. The results of the comparison, summarized in Table 4, show that there is a good agreement between the two methods in both insulated and uninsulated conditions. The percent error is very low, which is acceptable within the engineering standards. In the uninsulated case, the outer wall temperature is 404 K in the analytical analysis, whereas the numerical simulation gives the outer wall temperature of 395 K, respectively. The difference in temperature resulting temperature difference of 9 K with a percentage error of 2.22%. This near coincidence proves that the assumptions that were made in the analysis, like the one-dimensional steady-state heat conduction and material homogeneity, are valid in the case of the furnace wall without insulation. This slight difference is due to numerical effects like the discretization of the mesh, heat conduction depending on the temperature of the material, and heat flow in three dimensions, are the effects that are captured in FEA model but are neglected in the analytical formulation. Both methods also hint clearly that, in the absence of insulation, a lot of heat is lost to the environment, resulting in high temperatures on the exterior and low thermal performance.

Table 4: Comparison of Analytical and FEA results.

Condition	Analytical Design (K)	Numerical Design (K)	Difference (K)	Error (%)
Without Insulation	404	395	9	2.2
With Insulation	356	326	30	8.42

In the insulated scenario, when a ceramic fiber layer of thickness 40 mm is incorporated, the analytical model estimates the temperature of the outer surface to be 356 K and the numerical model estimates a lower temperature of 326 K, with a temperature difference of 30 K and a percentage error of 8.42%. Despite the fact that the deviation is larger than the uninsulated one, it still falls within a reasonable range of considerations in thermal design. The larger difference because the analytical model used simple assumptions including constant thermal conductivity and one-dimensional heat flow as opposed to the numerical model which considers more complicated heat transfer processes, including multi-dimensional conduction, interface effects, and increased convective and radiative losses at material boundaries. Notably, the both techniques show a considerable decrease in heat loss which proves the efficiency of ceramic fiber to raise thermal resistance.

On the whole, the comparison proves the fact that the analytical model gives a stable and conservative estimation, whereas the numerical model is a more realistic representation of the real operating conditions. The same pattern of the constant rate of high heat loss without insulation and high rates of heat retention with insulation in both analyses clearly shows that the use of 40mm ceramic fiber insulation can greatly enhance the performance of the furnace in terms of heat loss to the environment by a large percentage and by retention of a large percentage of heat inside the heating chamber. Such congruence between analytical and numerical findings proves the effectiveness of the furnace design and leads to its practical application.

Discussion

As shown in the comparative analysis in Table 5, most of the current research is mainly aimed at large-scale electric arc furnaces, and it is concerned with arc behavior, cooling methods and superior control methods. An example is the study by Al-Nasser et al. (2021) and Wang et al. (2025), which focus on arc dynamics and industrial-scale CFD modeling, and Babadi et al. (2023) and Assad et al. (2021), whose results are about the cooling improvement using nanofluids and material changes. These strategies are effective in lowering the surface temperatures or enhancing the ability to control operations; however, they are not paying much attention to the core of passive thermal efficiency enhancement by insulation or optimization of the structural design. Moreover, a number of

studies are based on sophisticated control systems (e.g., PID-based techniques) or computationally expensive models, which make systems more expensive and restrict their real-world use, especially in a laboratory-scale or small industrial environment.

Table 5: Comparison of the present research with previous studies.

Study	Furnace Type & Parameters Considered	Key Findings	Research Gap / Contribution of the Present Study
Al-Nasser et al. (2021)	Electric Arc Furnace; arc current, gas density, arc gap	Arc current strongly influences penetration and mixing	Does not address thermal efficiency or insulation; present study focuses on heat retention and safety.
Assad et al. (2021)	EAF roof; thermal conductivity, cooling design	Lower conductivity reduces surface temperature	Focus limited to cooling; present study improves insulation and internal heat retention.
Babadi et al. (2023)	EAF cooling panels; nanofluid concentration	14.4% reduction in wall temperature	Only cooling enhancement studied; present work improves energy efficiency via insulation.
Chen et al.(2024)	Hot metal system; slag thickness, ambient conditions	Slag significantly reduces heat loss	Not focused on furnace design; present study improves furnace wall performance directly.
Guney et al. (2025)	Electric furnace; PID control, multi-surface heating	High temperature uniformity with control systems	Requires complex control; present study achieves uniformity via geometry and insulation.
Huzaidi et al. (2023)	Lab furnace; heating elements, system redesign	Rapid heating to 650°C in 5–7 minutes	Limited temperature range; present study operates up to 1200°C
Li et al. (2024)	Vacuum furnace; thermal modeling, structural optimization	Validated model with <4% error	Complex vacuum system; present study offers simpler lab-scale solution.
Wang et al. (2025)	Industrial EAF; CFD modeling, melting process	Accurate industrial-scale predictions	High complexity and cost; present study is low-cost and experimentally feasible.
Present Study (2026)	Electric resistance furnace; insulation thickness, heat transfer, temperature distribution	45% heat loss reduction; uniform temperature distribution; safe external temperature; 1200°C operation	Provides validated analytical + FEA model, low-cost design, improved thermal efficiency, and practical lab-scale applicability.

Conversely, the current research fills these gaps through the consideration of a lab-scale electric resistance furnace and placing more stress on the combination of analytical modeling and finite element analysis to validate the study. The findings show that the amount of heat loss (reduced by an average of 45 per cent) can be minimized by adding ceramic fiber insulation, and the thermal homogeneity can be enhanced by a hexagonal chamber geometry. The suggested design is cost-effective as well as practical in comparison to other designs, as opposed to the earlier ones, as it does not rely on sophisticated control systems or costly cooling systems. Also, the analytical and numerical results are very close (within reasonable engineering tolerances), which validates the correctness of the suggested method. Thus, the research adds a simplified but useful design approach that increases thermal efficiency, safety in operation, and offers a scalable solution to high-temperature laboratory and small-scale industrial uses. Moreover, the current research proves that the attentive combination of the material choice, insulation, and chamber geometry can

dramatically improve the performance of the furnace without complicating the system. Ceramic fiber insulation, along with a hexagonal form, can be used to reduce the amount of heat loss as well as provide a more even distribution of temperature in the heating chamber. This points out to the fact that passive design techniques can be optimized to be an adequate ability that supplements or even overtakes active control options in some applications, and therefore the proposed system is very appropriate in the case of educational laboratories and small-scale thermal processing, where simplicity, dependability, and economic factors are paramount.

Conclusion

The assumptions and calculations testify that the project furnace design has a good thermal performance with proper insulation. The ANSYS APDL analysis of the finites elements reveals that, in the absence of insulation, a lot of heat is lost through the wall of the furnace leading to high and dangerous exterior temperature. A 40 mm thick ceramic fiber insulation layer is introduced to the product which has a considerable increase in its thermal resistance, decreasing heat loss to the environment, and keeping the outside surface near ambient temperature with high temperatures retained in the heating cavity. The uniformity of the heat distribution within the heating chamber of hexagonal shape is further deprived through the examples of numerical simulations carried out in ANSYS Workbench, which show a stable and effective thermal behavior. The cumulative output reveals that the furnace has a potential of reaching an interior temperature of about 1200 °C in about one hour with proper heat retention and enhanced safety in its use. In operating temperatures over 1200 °C, the data points to the fact that a greater insulation thickness is needed, and at temperatures over 1000 °C, Kanthal heating elements are suggested because of their better thermal stability and oxidation capability. Furthermore, integrating coupled thermal fluid analyses and performing validation under diverse operating conditions would provide deeper insights and support optimized design for high-temperature applications.

References

Al-Nasser, M., et al., Toward a simplified arc impingement model in a direct-current electric Arc Furnace. *Metals, 2021. 11*(9): p. 1482.

Abadi, M.M., H. Tang, and M.M. Rashidi, A review of simulation and numerical modeling of electric arc furnace (EAF) and its processes. *Heliyon, 2024. 10*(11).

Assad, M.E.H., et al., Numerical Investigation of Heat Transfer Water-Cooled Roof in an Electric Arc Furnace. *Journal of Thermal Engineering, 2021. 7*(3): p. 623-634.

Babadi Soultanzadeh, M., et al., Numerical investigation of nanofluid heat transfer in the wall cooling panels of an electric arc steelmaking furnace. *SN Applied Sciences, 2023. 5*(4): p. 99.

Chen, W., et al., Numerical Study on Heat Transfer Characteristic of Hot Metal Transportation before EAF Steelmaking Process. *Metals, 2024. 14*(6): p. 673.

Du, X., Z. Zhang, and S. Zhang, Current Status and Prospects of Electric Furnace Scrap Steel Preheating Technology. *International Core Journal of Engineering, 2025. 11*(6): p. 348-354.

Ferber, N.L., et al., Development of an electric arc furnace steel slag-based ceramic material for high temperature thermal energy storage applications. *Journal of energy storage, 2022.* 51: p. 104408.

Guney, A. and O. Cakir, Design and Real-Time Control of an Electric Furnace with Three-Dimensional Heating. *Electronics, 2025. 14*(3): p. 602.

Hussein, M.M., et al., Modern temperature control of electric furnace in industrial applications based on modified optimization technique. *Energies, 2022. 15*(22): p. 8474.

Huzaidi, M.N. and A.N. Paimin, Improvement of Electric Furnace Heating Function for Use in Aluminium Waste Management. *Research and Innovation in Technical and Vocational Education and Training, 2023. 3*(2): p. 112-121.

Hay, T., et al., Calculation of view factors in electric arc furnace process modeling. *Steel Research International, 2021. 92*(2): p. 2000341.

Jawahery, S., et al., Thermophysical model for online optimization and control of the electric arc furnace. *Metals, 2021. 11*(10): p. 1587.

Kishore, K., M.N. Sheikh, and M.N. Hadi, A critical analysis of electric arc furnace (EAF) slag for sustainable geopolymer concrete production. *Materials Today Sustainability, 2025*. 29: p. 101064.

Li, M., et al., Numerical simulation of the heating process in a vacuum sintering electric furnace and structural optimization. *Scientific Reports, 2024.* 14(1): p. 30905.

Lee, J., et al. Power Consumption Optimization for Electric Arc Furnace with Time Series Prediction. *In PHM Society Asia-Pacific Conference. 2023.*

Makarov, A.N., Theory and Practice of Heat Transfer in Electric Arc and Flare Furnaces and Power Plants. *World Journal of Engineering and Technology, 2020. 8*(04): p. 739.

Pauna, H., et al., Hydrogen Direct Reduced Iron Melting in an Electric Arc Furnace: Benefits of In Situ Monitoring. *Journal of Sustainable Metallurgy, 2025. 11*(4): p. 4655-4667.

Rinne, M., et al., Alternative method for treating electric arc furnace dust: simulation and life cycle assessment. *Journal of Sustainable Metallurgy, 2022. 8*(2): p. 913-926.

Varga, A., et al., Modeling of Heat Flux in a Heating Furnace. *Computation, 2023. 11*(7): p. 144.

Wang, S., et al., Computational Fluid Dynamics Simulation of Industrial Electric Arc Furnace Operation: Validation and Performance of Melting Phenomena. *Steel Research International, 2025. 96*(7): p. 2400509.